Magnetic x-ray spectroscopy of two-dimensional CrI_3 layers

Andreas Frisk[a], Liam B. Duffy[b,c], Shilei Zhang[c], Gerrit van der Laan[a], Thorsten Hesjedal[c,*]

[a] *Magnetic Spectroscopy Group, Diamond Light Source, Didcot, OX11 0DE, United Kingdom*
[b] *ISIS, STFC, Rutherford Appleton Lab, Didcot, OX11 0QX, United Kingdom*
[c] *Department of Physics, Clarendon Laboratory, University of Oxford, Oxford, OX1 3PU, United Kingdom*

Abstract

The recently confirmed monolayer ferromagnet CrI_3 is a frisky example of a two-dimensional ferromagnetic material with great application potential in van der Waals heterostructures. Here we present a soft x-ray absorption spectroscopy study of the magnetic bulk properties of CrI_3, giving insight into the magnetic coupling scenario which is relevant for understanding its thickness-dependent magnetic properties. The experimental Cr $L_{2,3}$ x-ray magnetic circular dichroism spectra show a good agreement with calculated spectra for a hybridized ground state. In this high-spin Cr ground state the Cr–I bonds show a strongly covalent character. This is responsible for the strong superexchange interaction and increased spin-orbit coupling, resulting in the large magnetic anisotropy of the two-dimensionally layered CrI_3 crystal.

Keywords: Magnetic materials, Spectroscopy, X-ray techniques

1. Introduction

CrI_3 belongs to the family of van der Waals materials [1] that is characterized by stacked two-dimensional (2D) layers which are weakly bonded together

*Corresponding author
Email address: Thorsten.Hesjedal@physics.ox.ac.uk (Thorsten Hesjedal)

(see Fig. 1(a,b)). Van der Waals heterostructures of 2D layers have a great potential for novel devices owing to the sheer endless number of possible materials combinations [2]. So far, the important magnetic members had been missing as ferromagnetism is not possible in isotropic 2D systems [3]. Monolayer CrI_3, on the other hand, is a 2D Ising ferromagnet with a magnetic ordering temperature of $T_C = 45\,K$ [1, 4], whereas bilayer CrI_3 is antiferromagnetic [1]. Trilayers (and above) show long-range ordered 3D ferromagnetism with $T_C = 61\,K$ [5]. In the ferromagnetic phase, CrI_3 is rhombohedral ($R\bar{3}$) (Fig. 1(a)) and it transforms into the monoclinic ($C2/m$) phase at $\sim$215 K (Fig. 1(b)) [6]. The 3D ferromagnetic behavior [5] highlights that the interlayer coupling between the 2D layers can not be ignored in bulk CrI_3. As a result, obtaining direct evidence for the mechanism behind the magnetic anisotropy and the intriguing behavior of 2D CrI_3 is a desirable, yet challenging task.

Here we report the determination of the magnetic ground state of CrI_3 using x-ray absorption spectroscopy (XAS) and x-ray magnetic circular dichroism (XMCD). These techniques offer the most direct way to determine the local electronic and magnetic structure of $3d$ transition metal atoms due to their valence-, site-, and symmetry-selectivity [7].

2. Experimental

2.1. Structural characterization

CrI_3 single crystals (HQ Graphene, Groningen, The Netherlands) have been characterized by room temperature x-ray diffraction (XRD) using Mo Kα ($\lambda = 0.7107\,$Å) and Cu Kα ($\lambda = 1.5418\,$Å) sources in a SuperNova single-crystal XRD system. At room-temperature, CrI_3 adopts the monoclinic $C2/m$ space group, and from single-crystal diffraction (Fig. 1(c)) we determined the lattice parameters to be $a = 6.87(4)\,$Å, $b = 11.89(7)\,$Å, $c = 6.98(3)\,$Å, and $\beta = 108.5(5)^\circ$, in agreement with Ref. [6].

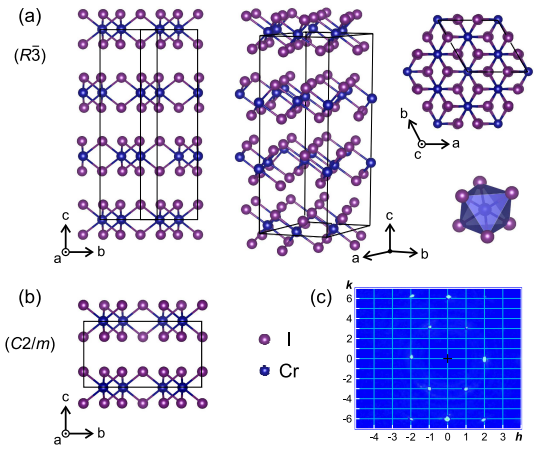

Figure 1: (a) Low-temperature crystal structure of CrI_3, viewed along the a-axis (left), perspective view (middle), and normal to the ab-plane (right). The I-Cr-I trilayers are separated by a van der Waals gap, and stacked along the c-axis direction. The Cr ions arrange in a hexagonal pattern. On the lower right, the coordination octahedron shows the Cr ion in the center of six I ions. (b) Room-temperature crystal structure ($C2/m$). (c) Single-crystal diffraction pattern showing the reciprocal space points in the ($hk0$) plane at room-temperature. A dashed grid in units of reciprocal lattice constants is shown for convenience.

2.2. X-ray magnetic circular dichroism

X-ray absorption spectra (XAS) at the Cr $L_{2,3}$ edges of freshly cleaved CrI_3 bulk samples were measured at 15, 50, and 300 K using the 14 T superconducting magnet on beamline I10 at the Diamond Light Source. XAS measurements were made in total-electron-yield mode, which is surface-sensitive with an exponentially decreasing probing depth of ∼4 nm [8]. The element-specific technique of x-ray magnetic circular dichroism (XMCD) is used to probe the magnetic ground state [9]. The XMCD spectrum is obtained as the difference between the two XAS spectra with the circular polarization vector parallel and antiparallel to the external magnetic field. Hence, the technique resemblances the magneto-optical phenomena in the visible region, such as the Faraday effect. Unlike the latter, the XMCD arises from the excitation of a core electron, instead of a valence electron, into the unoccupied conduction states. A field of

2 T was applied during the measurements which were performed with the field parallel to the x-ray beam at an incident angle of 30° relative to the surface normal. During the change between different temperatures, and for the initial cool down, no magnetic field was applied.

3. Results and discussion

Figure 2 shows the experimental XAS and XMCD spectra of CrI_3. At 15 and 50 K, i.e., below T_C, CrI_3 is in the long-range ordered ferromagnetic phase, and at 300 K it is paramagnetic. The XAS spectra shown in Figs. 2(a) and 3(a) are the averaged data obtained for left- and right circularly polarized light. The XAS measurements at the Cr $L_{2,3}$ edges show a similar lineshape of the spectra taken at 15 K and 50 K, and more pronounced features at 300 K. Note that the broader structure at 577 eV is due to some oxidation of Cr in the freshly cleaved samples. The XMCD spectra show strong dichroism in the ferromagnetic phase, and a vanishing signal in the paramagnet phase. An energy splitting between the two negative Cr L_3 peaks is found.

The measured Cr $L_{2,3}$ XAS and XMCD of CrI_3 (Fig. 3) are rather different from those of Cr-doped Bi_2Se_3 [10] and Sb_2Te_3 [11]. However, in some aspects the XAS of CrI_3 resembles that of the common oxide Cr_2O_3 [12], which is antiferromagnetic and thus has no XMCD. Instead, we can compare with the ferrimagnetic spinel $FeCr_2O_4$ [13] or Cr-doped magnetite [14], which has quite a different XMCD as that shown in Fig. 3. Thus, the XAS suggests a partial oxidization, whereas the XMCD is still mostly from the remaining CrI_3. It is also similar to that of $FeCr_2Se_4$ [15], which is mainly high-spin trivalent Cr with three electrons in the t_{2g} state. Its difference with Cr_2O_3 demonstrates that the character of the Cr–I bond is not simply ionic, but covalent.

Atomic multiplet theory is employed to calculate the Cr $L_{2,3}$ XAS and XMCD spectra using the electric-dipole transitions $3d^n \rightarrow 2p^5 3d^{n+1}$, where the spin-orbit and electrostatic interactions are treated on an equal footing [8]. The wave functions of the initial- and final-state configurations are calculated

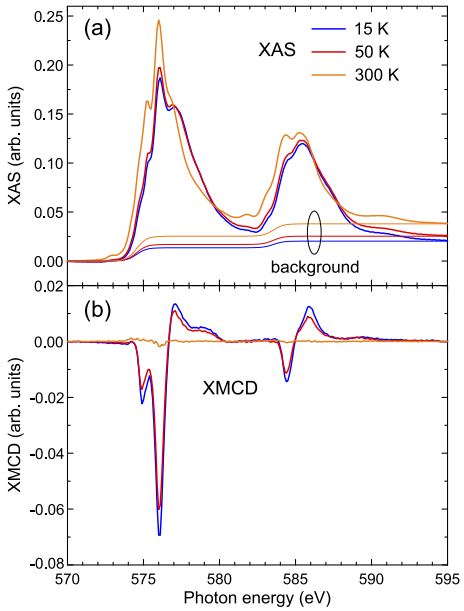

Figure 2: Temperature-dependent XAS and XMCD measurements of CrI_3 at the Cr $L_{2,3}$ edges in a field of 2 T. (a) Normalized XAS spectra (integral of the background subtracted-spectra set to one). (b) Corresponding XMCD signals.

in intermediate coupling using Cowan's atomic Hartree-Fock (HF) code with relativistic corrections [7, 16]. The atomic electrostatic interactions include the 3*d*-3*d* and 2*p*-3*d* Coulomb and exchange interactions, which are reduced to 80% and 75%, respectively, of their atomic HF value to account for the intra-atomic screening [8]. Hybridization effects are included by mixing the Cr $3d^3$ with $3d^4\underline{L}$ configurations, where $\underline{L}$ represents a hole on the neighboring atoms in states of appropriate symmetry. The charge-transfer energies in the initial- and final-state are $E(3d^4\underline{L}) - E(3d^3) = 1\,\text{eV}$ and $E(2p^5 3d^5\underline{L}) - E(2p^5 3d^4) = -1\,\text{eV}$, respectively. The hybridization parameter $T = \langle\psi(d^3)|H|\psi(d^4\underline{L})\rangle = 2\,\text{eV}$. The Cr L_3 (L_2) line spectra are broadened by a Lorentzian with a half-width of $\Gamma = 0.2\,\text{eV}$ (0.4 eV) for the intrinsic lifetime broadening and a Gaussian with a standard deviation of $\sigma = 0.15\,\text{eV}$ for the instrumental broadening.

By comparing with the experimental spectra, the ground state for Cr is ob-

tained as a hybridized state with 59% d^3 and 41% d^4 character in an octahedral crystal-field of $10\,Dq = 1.8\,\mathrm{eV}$, which corresponds to a d count of $n_d = 3.41$. This ground state has an orbital moment $m_L = -0.067\,\mu_\mathrm{B}/\mathrm{Cr}$ and an effective spin moment $m_S = 2.87\,\mu_\mathrm{B}/\mathrm{Cr}$ (i.e., $0.84\,\mu_\mathrm{B}$ per $3d$ electron). Figure 3 shows the excellent agreement between experimental and theoretical spectra.

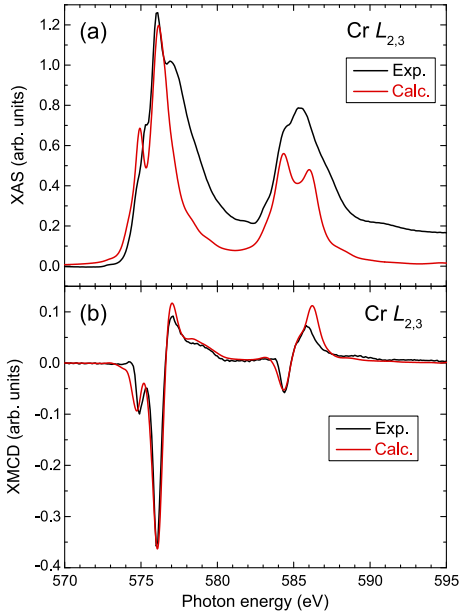

Figure 3: Experimental (black lines) Cr $L_{2,3}$ XAS and XMCD of CrI_3 film measured at 50 K and 2 T. Calculated (red lines) averaged XAS and XMCD spectra for a hybridized Cr ground state with 59% d^3 and 41% d^4 character in octahedral symmetry (see text for further details).

Our findings support recent theoretical work [17] which concludes that the Cr-I-Cr superexchange interaction is ferromagnetic. Comparing the related Cr halogenides $CrCl_3$, $CrBr_3$, and CrI_3, triiodide has the highest T_C despite the increased Cr-Cr distance resulting from the increased ionic radius in the halogen series [6]. On the other hand, the bonds with Cr become more covalent in the halogen series, leading to a stronger superexchange interaction and therefore higher T_C, as well as stronger spin-orbit coupling which is most likely responsible for the important magnetic anisotropy [17].

4. Conclusion

In summary, we performed magnetic spectroscopy on freshly cleaved CrI_3 crystals at temperatures above and below the magnetic ordering temperature. Below T_C, the experimental Cr $L_{2,3}$ XMCD spectra show a good agreement with calculated spectra for a hybridized ground state. In this high-spin Cr ground state with three electrons in the t_{2g} state, the Cr–I bonds show a strongly covalent character. Our experimental results therefore confirm the theoretical claim [17] that the increased covalent bonding in CrI_3, together with an increase in spin-orbit coupling, is responsible for the large magnetic anisotropy that is behind the 2D Ising behavior of monolayer CrI_3 [1].

Acknowledgements

Beamtime awarded on I10 at the Diamond Light Source (SI-16162) is acknowledged. A.F. acknowledges funding by EPSRC (EP/P021190/1), and L.B.D. was supported by STFC and an EPSRC DTG.

References

[1] B. Huang, G. Clark, E. Navarro-Moratalla, D. R. Klein, R. Cheng, K. L. Seyler, D. Zhong, E. Schmidgall, M. A. McGuire, D. H. Cobden, W. Yao, D. Xiao, P. Jarillo-Herrero, X. Xu, Nature 546 (2017) 270–273.

[2] A. K. Geim, I. V. Grigorieva, Nature 499 (2013) 419–425.

[3] N. D. Mermin, H. Wagner, Phys. Rev. Lett. 17 (1966) 1133–1136.

[4] R. B. Griffiths, Phys. Rev. 136 (1964) A437–A439.

[5] Y. Liu, C. Petrovic, Phys. Rev. B 97 (2018) 014420.

[6] M. A. McGuire, H. Dixit, V. R. Cooper, B. C. Sales, Chem. Mater. 27 (2015) 612–620.

[7] G. van der Laan, B. T. Thole, Phys. Rev. B 43 (1991) 13401–13411.

[8] B. T. Thole, G. van der Laan, J. C. Fuggle, G. A. Sawatzky, R. C. Karnatak, J. M. Esteva, Phys. Rev. B 32 (1985) 5107–5118.

[9] G. van der Laan, A. I. Figueroa, Coord. Chem. Rev. 277–278 (2014) 95–129.

[10] A. I. Figueroa, G. van der Laan, L. J. Collins-McIntyre, S.-L. Zhang, A. A. Baker, S. E. Harrison, P. Schönherr, G. Cibin, T. Hesjedal, Phys. Rev. B 90 (2014) 134402.

[11] L. B. Duffy, A. I. Figueroa, L. Gładczuk, N.-J. Steinke, K. Kummer, G. van der Laan, T. Hesjedal, Phys. Rev. B 95 (2017) 224422.

[12] C. Theil, J. van Elp, F. Folkmann, Phys. Rev. B 59 (1999) 7931–7936.

[13] J.-S. Kang, J. Hwang, D. H. Kim, E. Lee, W. C. Kim, C. S. Kim, H.-K. Lee, J.-Y. Kim, S. W. Han, S. C. Hong, B. Kim, B. I. Min, J. Appl. Phys. 113 (2013) 17E116.

[14] N. D. Telling, V. S. Coker, R. S. Cutting, G. van der Laan, C. I. Pearce, R. A. D. Pattrick, E. Arenholz, J. R. Lloyd, Appl. Phys. Lett. 95 (2009) 163701.

[15] J.-S. Kang, G. Kim, H. J. Lee, H. S. Kim, D. H. Kim, S. W. Han, S. J. Kim, C. S. Kim, H. Lee, J.-Y. Kim, B. I. Min, J. Appl. Phys. 103 (2008) 07D717.

[16] R. D. Cowan, The Theory of Atomic Structure and Spectra, University of California Press, Berkeley, 1992.

[17] J. L. Lado, J. Fernández-Rossier, 2D Mater. 4 (2017) 035002.